Solar wind bremsstrahlung off dark matter in our Solar System

Gilles Couture

Département des Sciences de la Terre et de l'Atmosphère, Université du Québec à Montréal, 201 Avenue du Président Kennedy, Montréal, Quebec H2X 3Y7, Canada

(Received 8 July 2021; accepted 3 January 2022; published 9 March 2022)

We consider the possibility that the solar wind emits photons via *bremsstrahlung* when colliding with dark matter particles within the Solar System. To this effect, we calculate the bremsstrahlung spectrum that a proton would emit when colliding with a neutral spin-1/2 particle through the exchange of a scalar neutral particle. We assume a speed of 600 km/sec for the solar wind and assume that the speed of the dark matter halo is due to the motion of the Sun through our Galaxy, which we take as 300 km/sec. We assume a dark matter density of 0.3 GeV/cm^3 and a solar wind composed primarily of protons with a total rate of ejection mass set at 10^9 kg/sec. We use a Monte Carlo technique to let this interaction take place within the Solar System and calculate the photon rate an observer would detect on Earth or at the edge of the Solar System as a function of photon energy. We find that the rates are in general very small but could be observable in some scenarios at wavelengths in the mm range at a telescope like ALMA; this could lead to interesting constraints on couplings and masses.

DOI: 10.1103/PhysRevD.105.055003

I. INTRODUCTION

About one year ago, Xenon1T reported a clean signal above known backgrounds [1]. This measurement triggered a flurry of activity aiming at explaining this signal in the context of dark matter (DM) [1–5] or others [6,7]. Xenon1T is one of several *direct detection* cryogenic detectors [8–13] where the DM particle interacts directly with the nucleus of the detector and one records its recoil [14–16]. There are also direct detectors where the energy deposited by the DM particles causes the explosion of a superheated droplet embedded in a gel and one simply records the sound wave [17–20]. The direct detection approach suffers from a mass threshold: when the mass of the DM particle becomes small, it becomes very difficult for the DM particle to deposit enough energy in the nucleus to produce a detectable signal. In order to overcome this low mass threshold, new mechanisms based on the Migdal effect use the effect of the recoil of the nucleus on the electronic cloud [21–30] or the bremsstrahlung photon that could result from this interaction [31]. Another avenue is to explore the possibility that the DM particles be upscattered by more energetic particles such as neutrinos [32] or cosmic rays [33,34].

The indirect detection approach relies on the gravitational pull of massive bodies that could lead to the accumulation of DM particles in their core, be they the Earth, the Sun or the Galaxy. This increase in density will lead to an enhanced probability of the annihilation of a DM particle antiparticle which would then produce standard particles that could be detected on Earth [35]. The presence of DM inside the Sun would have an effect on its behavior and some interesting limits on axion-photon couplings have been obtained from a global fit to solar data, including helioseismology [36]. Allowing both the accumulation of DM particles inside the Sun and their interaction with electrons would lead to DM upscattering off the electrons and possibly interesting rates on Earth of DM energetic enough to produce a signal in the direct detection experiments [37]. A similar accumulation could take place within exoplanets and would affect their evolution [38].

The presence of DM in the early Universe will also have an effect on its early evolution [39] and could produce a distortion in the cosmic microwave background at recombination [40] as well as affecting the evolution of galaxies and their satellites later on [41].

Recently, an Earth-scale detector called GNOME [42] reported a first null result from a relatively short operation time aiming at measuring a topological defect due to an axionlike particle field propagating through space [43]. The signal from such a field as the Earth crosses it would be a slight perturbation in high precision/sensitivity instruments such as atomic clocks occurring at slightly different instants.

DM particles could also be produced at high energy colliders such as the LHC [44,45].

In this paper, we calculate the bremsstrahlung photon flux one would receive from the collision between a proton

from the solar wind and a DM particle in the vicinity of the Solar System. We consider space itself as a collider whose collision angle and luminosity will vary throughout the Solar System. We neglect cosmic magnetic fields and assume that the solar wind travels in straight line at a speed of 600 km/ sec ($\beta_M = 0.002$). We consider that protons constitute most of the solar wind and the ejection mass rate from the Sun is set at 10^9 kg/ sec $= \mathcal{R}_{sw}$. We assume that the dark matter has a density of 0.3 GeV/cm^3 [46–48] and that it is at rest in our part of the Galaxy; its relative motion is due to the motion of the Sun, which we take as 300 km/ sec ($\beta_{\rm DM} = 0.001$).

In the following sections, we describe some technical points before presenting our results and conclusions.

II. PROCEDURE

The process we are interested in is

$$p(p) + q(q) \to p(\bar{p}) + q(\bar{q}) + \gamma(k), \tag{1}$$

where p is the proton, q is the DM particle and γ is the photon. As it is a three-body final sate, we will use a Monte Carlo technique to calculate this spectrum.

Bremsstrahlung has been studied by Bethe and Heitler in the context of a charged particle colliding with a much more massive particle; for example, a proton impinging on a heavy nucleus [49,50]. This process is still of interest as higher corrections are added to the original work [51–56]. Processes where a hard photon is produced through the interaction of a particle with a DM particle have been studied recently [57,58], but the bremsstrahlung we study here is a little different in that it is due to the exchange of a light neutral particle. When a proton collides with an atom, it does not feel an important positive charge until it is well inside the electronic cloud and feels the full nuclear electric charge when it is inside the innermost electronic shell. This takes place at a distance that is less than 0.053 nm since the average value of r is $\frac{a_0}{2Z}(3n^2 - l(l+1))$. With DM, it does not see the object until it is within the range of the messenger scalar, which is about 2×10^{-15} m for a messenger of 0.1 GeV.

In order to calculate the photon flux, we will proceed as follows:

(1) Using a Monte Carlo technique based on the matrix element of the process at hand, we build the distribution $d^2\sigma/dE_\gamma d\cos\theta_\gamma$ for several collision angles between the proton and the DM particle.
(2) We pick an observation point with an observation cone of a given opening angle and orientation: we will consider two observation points and four orientations.
(3) Using a Monte Carlo technique, we scan the observation cone in a random and uniform way. Each observation point within this cone defines completely all angles and distances of the collision.
(4) Since we have calculated $d^2\sigma/dE_\gamma d\cos\theta_\gamma$ for that given colliding angle and outgoing photon angle, we select σ at random within the distribution and read the corresponding E_γ for this event.
(5) Multiplying this partial cross section by the luminosity $\mathcal{L}$ at that position and different geometrical parameters that take into account the fact that the photon can be emitted anywhere on a cone of angle θ_γ and will not necessarily reach the Earth, we obtain Φ_γ and E_γ for this event.
(6) Averaging the distribution produced within the cone and multiplying by the number of independent colliders in the cone, given by $V_{\rm cone}/V_{\rm accelerator}$, will give the desired flux.

We set our axes such that the Sun is at the origin, the Earth is along the positive y axis and its rotation around the Sun is from the positive x to the positive y axes.

III. MATRIX ELEMENT

We consider a relatively simple, generic model where a proton scatters off a neutral spin-1/2 DM particle through the exchange of a scalar neutral DM particle. We set the mass of the proton at 1 GeV. The DM masses and the couplings are free: $p - p - DM_{\rm exchange} = \lambda$ and $DM_{\rm collide} - DM_{\rm collide} - DM_{\rm exchange} = \Lambda$, where $DM_{\rm collide}$ is the DM particle that collides with the proton and $DM_{\rm exchange}$ is the DM particle exchanged between the proton and the $DM_{\rm collide}$ particle. Since we do not take into account the spin of the proton, the only angles that can be defined in the process are with respect to $\vec{\beta}_M$: $\theta_{\rm DM}$, the angle between the incoming proton and the DM particle, and θ_γ, the angle of the outgoing photon with respect to the incoming proton, are the relevant angles of the process since we do not observe neither the proton nor the DM particle after the collision.

As the speeds of the colliding particles are small, we have a nonrelativistic problem where the maximum energy of the photon is

$$E_\gamma^{\rm max} = \frac{(1/2)(M_M M_{\rm DM})(\vec{\beta}_M - \vec{\beta}_{\rm DM})^2}{M_M + M_{\rm DM}}, \tag{2}$$

where M as a subscript stands for *matter* or *proton* in our case.

We are mostly interested in the low energy part of the photon spectrum: the eV and sub-eV scale. As is well known [59–61], bremsstrahlung processes tend to diverge if we let the energy of the photon go to 0, the divergencies being canceled by the higher order corrections. In our case, we set the minimal energy of the photon at 10^{-10} GeV. The null mass of the photon is potentially a numerical problem; in order to avoid numerically negative photon masses and

instabilities, we give a mass to the photon ($k^2 = m_\gamma^2$) and include the extra terms in the matrix element that come with this mass: the summation over polarization states is $(g^{\mu\nu} - k^\mu k^\nu / m_\gamma^2)$. We have verified that masses between 10^{-13} and 10^{-16} GeV give identical results, but a mass of 10^{-11} GeV does not; we worked with 10^{-14} GeV.

At this point, when considering a head-on collision process and varying the incoming energies of the colliding particles, we observe the usual behavior of bremsstrahlung photons as having a slightly enhanced emission probability at a right angle at low energy and peaking more and more in the forward direction at higher energies.

IV. MONTE CARLO TECHNIQUE

Clearly, in the process that we want to study, the solar wind will not be in a head on collision with the DM. We then modify the boost factor of our center of mass system (CM) to take into account the angle of incidence of the DM [50,62,63]. In every collision, the motion of the solar wind particle defines our positive z' axis. The angle between the matter particle and the DM particle $\theta_{\rm DM}$ is defined such that a head-on collision corresponds to $\theta_{\rm DM} = 0$ and collinear collision corresponds to $\theta_{\rm DM} = 180$. We then consider a boost factor at a given angle $\theta_{\rm DM}$:

$$\vec{\beta}_{\rm CM} = (-q_{x'}, -q_{y'}, p_{z'} - q_{z'})/(p^0 + q^0) \tag{3}$$

and

$$\chi_{\rm CM} = (1/2)\log((1+\beta_{\rm CM})/(1-\beta_{\rm CM})), \tag{4}$$

where χ is the rapidity factor of the process. The Mandelstam variable $s \equiv (p+q)^2$ becomes

$$s = M_M^2 + M_{\rm DM}^2 + 2M_M M_{\rm DM}\gamma_M\gamma_{\rm DM}(1+\beta_M\beta_{\rm DM}\cos(\theta_{\rm DM})), \tag{5}$$

where γ_M and $\gamma_{\rm DM}$ are the usual relativistic parameters.

Taking these into account, we use a Monte Carlo technique to build the different distributions. The distributions are $d\sigma/d\cos(\theta_\gamma), d\sigma/dE_\gamma$ and $d^2\sigma/d\cos(\theta_\gamma)dE_\gamma$; where E_γ is the energy of the emitted photon and θ_γ is the photon angle with respect to the positive z' axis, i.e., the incoming matter particle. The energy distribution converges very smoothly, but the angular distribution, due to the three-body final state, is slower to converge and required 2×10^9 events to reach a relatively clean distribution. There was still a fairly large spread in the amplitude of the angular distributions and we used a fifth-order smoothing algorithm [64]:

$$y_i = \frac{1}{35}(-3y_{i-2} + 12y_{i-1} + 17y_i + 12y_{i+1} - 3y_{i+2}). \tag{6}$$

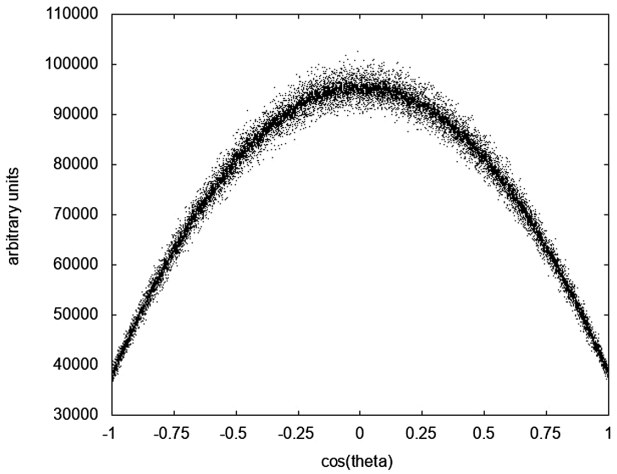

FIG. 1. Angular distribution before and after smoothing; the narrow band is the final distribution.

After 150 iterations, the spread is reduced by about a factor 5 and keeps the general features of the original distribution as can be seen on Fig. 1 where the narrow band is the final distribution.

The doubly differentiated distribution $d^2\sigma/d\cos(\theta_\gamma)dE_\gamma$ is the most important in what follows. In order to study the interaction of the solar wind with the DM halo, we built this distribution for collision angles ($\theta_{\rm DM}$) from 0° to 180° by increments of 10°; we have then 19 distributions.

V. SCANNING THE SOLAR SYSTEM

Once we have these distributions, we let the solar wind scatter off the DM in the Solar System and beyond. We first pick an observation point from which originates an observation cone of a given opening angle (δ_C), length and orientation; all photons observed must be produced within this cone. Once we have picked a collision point at random within the cone, all angles and distances are well defined: $\theta_{\rm DM}$, θ_γ, $\vec{R}$ (the vector from the observation point to the collision point) and $\vec{D}$ (the vector from the Sun to the collision point).

We build the photon flux (Φ in $1/{\rm m}^2$ sec) as

$$\frac{d\Phi}{dE_\gamma} = \frac{1}{N}\left\langle\frac{d\Phi}{dE_\gamma}\right\rangle\left(\frac{V_{\rm cone}}{V_{\rm collider}}\right), \tag{7}$$

where

$$\left\langle\frac{d\Phi}{dE_\gamma}\right\rangle = \left(\sum_{i=1}^{N}\left(\frac{d^2\sigma}{d\cos(\theta_\gamma)dE_\gamma}\right)_i \cdot G_i\right)\Bigg|_{\substack{\cos(\theta_\gamma)_i = \\ \cos(\theta_\gamma^{\rm Earth})_i}}\Bigg|_{\hat{r}_i\in{\rm cone}} \tag{8}$$

and

$$G_i = \frac{(\Delta\cos(\theta_\gamma))_i \mathcal{L}_i}{2\pi(R\sin(\theta_\gamma))_i (R\Delta\theta_\gamma)_i}. \quad (9)$$

$\mathcal{L}_i$ is the luminosity at the colliding point, $\hat{r}_i$ is a unit vector from the observation point to the colliding point, $\Delta\cos(\theta_\gamma)$ is the width of the bin previously defined, and $\Delta\theta_\gamma$ is the angular width of the band that we consider at the Earth. G_i takes into account the fact that the photon is emitted on a cone of angle $(\theta_\gamma)_i$ and will not necessarily reach the Earth. Once the cone has been sampled and averaged, we multiply by the number of independent accelerators that we have in our cone.

The Sun is at the origin of our coordinate system and our observation point is along the positive y axis; this is $\vec{R}_o$. We define the elevation angle of the observation apparatus as θ above the ecliptic plane and ϕ from the positive y axis towards the positive x axis. The aperture of the observing apparatus defines the opening angle of the observing cone; δ_C such that the total angle of the cone is $2\delta_C$. We will use $\delta_C = 40°$.

In order to sample the cone in a uniform and random manner, we embed the cone in a cube (x'', y'', z'') tailored to the cone and produce random numbers within each axis of the cube. We keep the events that fall within the cone and do not take into account those that lay outside of our cone. Due to the $1/D^2$ behavior of the solar flux that will appear later in the luminosity and the $1/2\pi R\,\sin\theta_\gamma\, R\,\Delta\theta_\gamma$ behavior of the area of the ring where the photon can be emitted, one expects that the contribution of very far away colliders will decrease and, therefore, when building our distributions, we should reach a plateau, a maximum photon flux once the length of our cone of integration reaches a certain value. Numerically, we should even observe a decrease in the amplitude of the distributions if we increase the length of the cone since integration up to very far distances would take a very large number of events in order to scan properly the regions that contribute most. We observe this behavior in our distributions. We should also observe an increase in the number of photons when we increase the opening angle of the observational cone; this relation is not so straightforward though as the emission of the bremmstrahlung photon is not uniform in the collision process and some regions of the observation cone might be better at producing photons than others. We also observe this behavior in our distributions.

In order to scan the cone, we proceed as follows: our observation point is at the origin of our $x'' - y'' - z''$ frame where we generate coordinates at random. This frame has the same orientation as our observation cone and its x'' axis corresponds to our x axis (we set $\phi = 0$). The cone is simply rotated by a certain angle around its x'' axis. Once the (x'', y'', z'') coordinates are generated at random, we have $\vec{R}$, the vector from the observation point to the colliding point. It is then straightforward to define the vectors that define the position of the observation point and the collision point. We consider four such rotations:

(1) 45°: we look 45° above the ecliptic with our back to the Sun.
(2) 90°: we look 90° above the ecliptic plane.
(3) 135°: we look 45° above the ecliptic plane and partly toward the Sun.
(4) 180°: we look directly at the Sun but we exclude a cone of 2° full angle in order to exclude the Sun itself.

The relevant vectors are then

$$\vec{R_o} = (0, R_o, 0), \qquad \vec{D} = \vec{R_o} + \vec{R},$$

$$\vec{V}_{\rm DM} = \beta_{\rm DM}(0, -1, 0), \qquad \vec{V}_M = \beta_M(D_x, D_y, D_z)/|\vec{D}|.$$

In this work, we assume that the DM is incoming along the $-y$ axis; the motion of the Sun is in the direction of the ecliptic plane towards the Earth. The angles $\theta_{\rm DM}$ and θ_γ are obtained from the scalar products

$$\cos(\psi) = \frac{\vec{D}\cdot\vec{V}_{\rm DM}}{DV_{\rm DM}} \quad \text{and} \quad \cos(\eta) = \frac{\vec{D}\cdot\vec{R}}{DR}$$

From these definitions we have $\theta_{\rm DM} = \pi - \psi$ and $\theta_\gamma = \pi - \eta$.

VI. PROBABILITY FOR THE OUTGOING PHOTON TO BE EJECTED WITH A GIVEN ENERGY

Once these angles are determined we go back to the distributions we built previously and pick the one that corresponds to the correct value of $\theta_{\rm DM}$; i.e., the $d^2\sigma/d\cos(\theta_\gamma)dE_\gamma$ that corresponds to our value of $\theta_{\rm DM}$. Within this distribution, we pick the specific row that corresponds to the correct value of θ_γ. This row represents the distribution $d\sigma/dE_\gamma$ for $\theta_{\rm DM}$ and θ_γ fixed by the position of the collision point. Within this distribution, we consider the highest possible value of the differential cross section and pick a number at random between 0 and 1 to multiply it with. Since the cross section (differential or total) represents the probability that a given process takes place, multiplying this maximum value by a random number between 0 and 1 will give the probability that the wanted process take place. We then read the corresponding value of the photon energy. We now have the cross section (or probability) that a photon be produced at a given angle with a given energy when a proton of a given energy collides with a DM particle of a given energy at a given incoming angle.

VII. LUMINOSITY

The luminosity ($1/\mathrm{m}^2$ sec) depends on the densities and velocities of the colliding particles and also on the colliding

angle [65,66] We assume a uniform density of the dark matter cloud within our region of the Galaxy and set it at 0.3 GeV/cm^3. Regarding the solar wind, we assume that the Sun emits a certain amount of material in space every second: we set it at 10^9 kg/ sec and assume that it is mostly protons. We also include the usual $1/D^2$ behavior of the solar flux, which leads to a decreasing density of the solar wind but we assume that this density is constant over the 600 km that our solar wind travels in one second. Essentially, we consider a beam of uniform density over 600 km in length and 1 meter in cross section. Since the interaction rate is rather small, we do not take into account the depletion of the solar wind flux as it travels through space. In these conditions, the required kinematical factor is given by

$$K = \sqrt{(\vec{\beta}_M - \vec{\beta}_{\rm DM})^2 - (\vec{\beta}_M \times \beta_{\rm DM})^2}, \tag{10}$$

so that the luminosity is given by

$$\mathcal{L} = \rho_M \rho_{\rm DM} L_x L_y v_M v_{\rm DM} \Delta t * K, \tag{11}$$

where L_x and L_y are the transverse sections of the *beam*, which we take as 1 m, and Δt is the timescale of the collision, which we take as 1 second. ρ_M is the density of matter (protons) at the collision point, given by

$$\rho_M = \frac{\mathcal{R}_{sw}/m_{\rm proton}}{4\pi D^2 v_M},$$

and $\rho_{\rm DM}$ is the density of dark matter particles at the collision point in $1/m^3$.

In order to get the final spectrum from this observation cone, we divide the distribution that we just built by the number of events used (which gives us the average spectrum) and then multiply by the number of independent accelerators within this cone: $V_{\rm cone}/V_{\rm collider}$. We take $V_{\rm collider} = (600000 + 300000)$ m^3. This procedure is justified since the distances travelled by our particles in 1 second are very much smaller than the distances at hand: we would need to consider $\sim 10^{28}$ collision points for our colliders to begin to overlap within the cone. This procedure is also symmetric both from the point of view of the matter and from the point of view of the DM particle. We neglect the effect encountered when $\theta_{\rm DM} = 180$, in which case the two volumes would overlap.

VIII. FREE PARAMETERS

There are five free elements in this scenario: two DM masses, two DM couplings and the density of DM particles in the Galaxy. Clearly, the couplings and the density of the DM particles in the Solar System simply factor out as $\rho_{\rm DM}$ and $\lambda^2\Lambda^2$. The mass of the DM particle exchanged in the process also factors out as $1/m^4$ since we have a t-channel process and the photon energies involved are much smaller than the masses. Regarding the mass of the incoming DM particle, it does not factor out and we find that the maximum bremsstrahlung occurs when its mass is about twice that of the proton so that the proton and the colliding DM particle have about the same momentum. The angle of the observation cone also factors out, but one has to be careful because the production volume might depend on the orientation when this angle becomes small. Therefore, our results can be scaled up or down by multiplying them by the following expression:

$$\frac{(\lambda^2\Lambda^2)\cdot(\rho_{\rm DM}/\rho^0_{\rm DM})\cdot(\mathcal{R}_{sw}/\mathcal{R}^0_{sw})\cdot(\tan(\delta_C)/\tan(\delta^0_C))^2}{(M_{\rm exchange}/0.1\ {\rm GeV})^4},$$

where $\mathcal{R}^0_{sw} = 10^9$ kg/ sec, $\rho^0_{\rm DM} = 0.3$ GeV/cm^3, $\delta^0_c = 40°$.

IX. RESULTS AND SIGNAL

We consider two observation points: one at 1 au (the Earth) and another at the edge of the Solar System, at 50 au (note that when looking directly at the Sun from 50 au, reducing the exclusion cone from 1°, as it was at 1 au to 1/50° has very little effect). We also consider two scenarios: in the first one (scenario A), the colliding DM particle has a mass of 2 GeV and the exchange particle has a mass 0.1 GeV. Such scenarios have been considered as *secluded weakly interacting massive particle dark matter* and some models allow excited state [67–69]. In the second scenario (scenario B), the colliding particle and the exchange particle have the same mass. In scenario A, we use the mass of the colliding particle to calculate the density of DM particles ($\rho_{\rm DM}$). We also considered several lengths and opening angles of the observational cone and verified that our distributions behaved as expected.

The result is Figs. 2–5, which represent $\frac{d\Phi_\gamma}{dE_\gamma}$ vs E_γ where $\frac{d\Phi_\gamma}{dE_\gamma}$ is in $1/{\rm m}^2$ sec eV and E_γ is in eV; recall that the visible spectrum is from 1.6 to 3.2 eV. One notes the following:

(1) All curves exhibit a straight line at low photon energy but show some noise at higher energy; the higher energy part of the spectrum converges more slowly. One obtains such straight lines from the classical Bethe-Heitler spectrum [50] if plotted on log-log axes.
(2) The rate at 45° is substantially smaller than the rates at 90°, 135° and 180°.
(3) The rates at 90°, 135° and 180° are very similar.
(4) All slopes at 1 au are very similar, at about -3.2 $1/{\rm m}^2$ sec eV^2, for both scenarios
(5) The slopes at a distance of 50 au are also very similar to those at 1 au.
(6) The rate at 50 au when looking at the Sun is similar to the rate at 1° au and 45° with a behavior similar to that of 1 au when the observation angle changes.

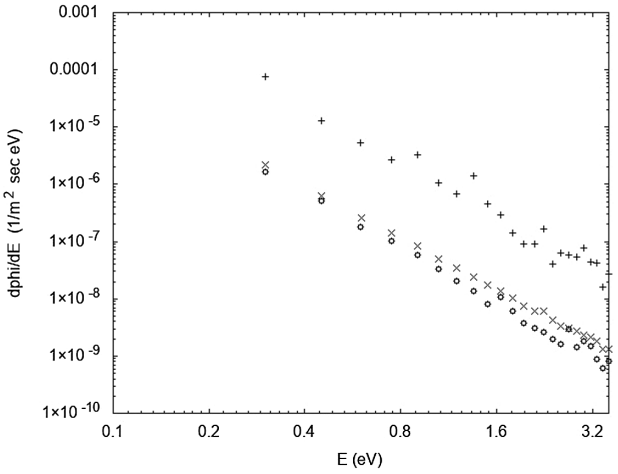

FIG. 2. Photon flux ($1/\mathrm{m}^2$ sec eV) vs photon energy (eV) for 1 au-180° (+), 1 au-45° (x), and 50 au-180° (o) in scenario A.

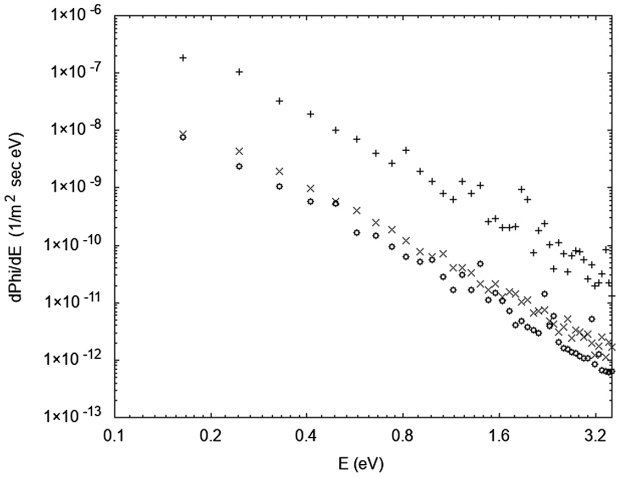

FIG. 4. Photon flux ($1/\mathrm{m}^2$ sec eV) vs photon energy (eV) for 1 au-180° (+), 1 au-45° (x) and 50 au-180° (o) in scenario B.

The straight lines indicate that

$$d\Phi(E_\gamma)/dE_\gamma = \Upsilon_0 (E_\gamma/E_\gamma^0)^{-\alpha} \rightarrow \tag{12}$$

$$\Phi|_{E_\gamma^{\min}}^{E_\gamma^{\max}} = \frac{\Upsilon_0 (E_\gamma^0)^\alpha}{\alpha - 1} \left\{ \frac{1}{(E_\gamma^{\min})^{\alpha-1}} - \frac{1}{(E_\gamma^{\max})^{\alpha-1}} \right\}, \tag{13}$$

where Υ_0 ($1/\mathrm{m}^2$ sec eV) and E_γ^0 is some reference point.

From Figs. 2–5, we can extrapolate safely to 0.01 eV and with caution somewhat below. Using these different parameters, we obtain Table I, where we give the photon flux ($1/\mathrm{m}^2$ sec) for different scenarios and photon energy bands. As we have already covered the whole observation cone, taking into account its opening angle of 40°, we could say that our units are $1/\mathrm{m}^2$ sec (0.47πsr). One has to be careful in scaling because opening or closing the observation cone at different observation angles might not give the same result as the productive zones may vary in size at different observation angles. From Table I, we can see that the rates are very small over the whole range with the parameters used here but could become interesting at wavelengths of mm (with energies in the meV range) in scenario A, where the mass of the colliding dark matter particle is about 2 GeV and the mass of the exchanged particle is about 0.1 GeV. Of course, there is a certain uncertainty in our extrapolations but we could say that in scenarios A-180-01 and A-135-01 we could expect a few 1000 photons $\mathrm{m}^{-2}\,\mathrm{sec}^{-1}$ at photon energies between 0.1 and 0.5 meV.

The processes studied here would translate into a diffuse background, without a precise source over a wide frequency range. Our calculations showed that the signal comes from a region that is relatively close to the Sun: about 50 au or less. Integrating beyond that point does not improve the photon flux observed on Earth and in fact degrades the curves because scanning properly the most

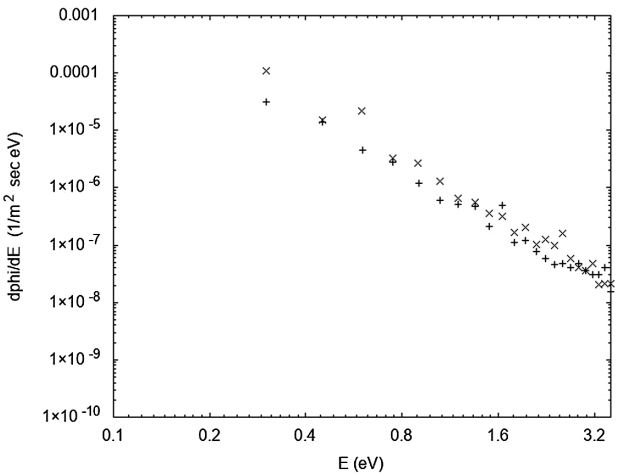

FIG. 3. Photon flux ($1/\mathrm{m}^2$ sec eV) vs photon energy (eV) for 1 au-90° (+), and 1 au-135° (x) in scenario A.

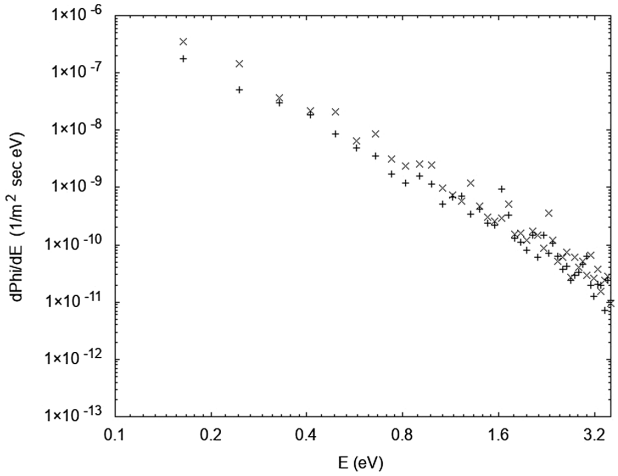

FIG. 5. Photon flux ($1/\mathrm{m}^2$ sec eV) vs photon energy (eV) for 1 au-90° (+), and 1 au-135° (x) in scenario B.

TABLE I. Integrated expected photon fluxes for the two scenarios considered, for different observation angles and for different energy bands. In scenario A, the colliding particle has a mass of 2 GeV while the exchange particle has a mass of 0.1 GeV, while both have a mass of 0.1 GeV in scenario B. A-180-01 means: scenario A, observation angle of 180° (directly at the Sun) and observation point at 1 au from the Sun. The fluxes are in $1/\mathrm{m}^2$ sec. If one takes into account that the opening angle of the observation cone is 40°, then our units for the flux are $1/\mathrm{m}^2$ sec $(0.47\pi\mathrm{sr})$.

Scenario	Slope	1.6–3.2 eV	0.5–1.0 eV	0.1–0.5 eV	10–50 meV	1–5 meV	0.1–0.5 meV
A-180-01	−3.38	9.5×10^{-8}	1.5×10^{-6}	8.4×10^{-5}	0.021	5.1	1200
A-135-01	−3.50	1.4×10^{-7}	2.6×10^{-6}	1.7×10^{-4}	0.053	17	5400
A-90-01	−3.10	1.0×10^{-7}	1.14×10^{-6}	4.2×10^{-5}	5.4×10^{-3}	0.68	86
A-45-01	−2.99	8.4×10^{-9}	8.6×10^{-8}	2.7×10^{-6}	2.6×10^{-4}	0.026	2.6
A-180-50	−3.28	4.5×10^{-9}	6.3×10^{-8}	3.0×10^{-6}	5.9×10^{-4}	0.11	22
B-180-01	−3.17	1.2×10^{-10}	1.5×10^{-9}	6.2×10^{-8}	9.1×10^{-6}	1.4×10^{-3}	0.20
B-135-01	−3.16	1.5×10^{-10}	1.8×10^{-9}	7.2×10^{-8}	1.0×10^{-5}	1.5×10^{-3}	0.21
B-90-01	−3.10	8.5×10^{-11}	9.7×10^{-10}	3.6×10^{-8}	4.6×10^{-6}	5.7×10^{-4}	0.072
B-45-01	−2.96	8.9×10^{-12}	8.7×10^{-11}	2.6×10^{-9}	2.4×10^{-7}	2.2×10^{-5}	0.002
B-180-50	−3.13	3.4×10^{-12}	4.1×10^{-11}	1.6×10^{-9}	2.1×10^{-7}	2.9×10^{-5}	0.004

productive volume requires more events as we scan the whole volume uniformly. Therefore, it would not be necessary to look very far into space to see our signal. When the observation point is at the edge of the Solar System (at 50 au, for example) we integrated up to 100–125 au. Such a diffuse signal could be difficult to detect and a plausible strategy could be to consider regions of the spectrum where there are no or very few known signals and/or backgrounds. Since we consider the Solar System as a collider, not only will the collision angle vary from one interaction point to another, but so will the luminosity. In these conditions, the cross section for a given colliding angle is not particularly useful, and the result that is more significant is the photon flux one could observe at a given observation point; as given in Table I.

An important parameter of our calculation is the angle of the cone of interaction, which is related to the field of view. For a regular telescope, the field of view has little effect on the number of photons that reach the telescope from a given star: a wider field of view will increase the number of stars seen by the telescope but not the number of photons from a particular star. In the process at hand however, the field of view is very important as space itself is the collider where the process takes place: the wider the field of view, the larger the cone of interaction is and the more photons can reach us. In our calculations, we used a large field of view with a cone of a semiangle of 40°; which translates into a solid angle of $0.47\pi \sim 1.48$ sr.

We will consider the configuration A-180-01, which is the observation of the sky on Earth and towards the Sun but excluding looking directly at the Sun. The situation is similar to that of looking at 45° from the Sun and the resulting photon fluxes are similar (A-135-01).

The New Horizon probe is now at roughly 50 au from the Sun and it has observed a diffuse background [70] in the visible, between 400 and 900 nm: the sky is a little brighter than it should be once all known sources and backgrounds are subtracted. The excess is about 17 ± 4 nW m^{-2} sr^{-1}, which translates into about $5.5 \pm 1.3 \times 10^{10}$ photons m^{-2} sec^{-1} sr^{-1} if we assume an average photon energy of 2 eV in the visible. If we consider the uncertainty as the lower limit of detection, we get 1.3×10^{10} photons m^{-2} sec^{-1} sr^{-1}. The process at hand would produce over the whole visible spectrum about 10^{-7} photons m^{-2} sec^{-1} with a field of view of 1.48 sr if the detector is on Earth and about 3×10^{-12} photons m^{-2} sec^{-1} if the detector is at 50 au and looks back at the Sun.

The VISIR [71] instrument at the VLT-ESO is sensitive to micron range and the user's manual states a wavelength of 8.7 micron with FWHM = 0.74 microns with filter J8-9 and a sensitivity of 4 mJy for 10 sigma. Clearly, 10 sigma is an excellent signal. If we go down to 3 sigma and an integration time of 8 hours, we could get 0.42 mJy. Remembering that a Jansky = Jy = 10^{-26} watt m^{-2} Hz^{-1}, this would translate into about 540 photons m^{-2} sec^{-1} between 8.33 and 9.07 microns to record a clean signal over the detection threshold. The field of view is rather small however with 3838 arcsec × arcsec → 3×10^{-8} sr. The process at hand would produce, between 0.1368 and 0.1490 eV about 7.5×10^{-6} photons m^{-2} sec^{-1} with a field of view of 1.48 sr.

The KEK instrument [72] is sensitive to the micron domain. We will use the quoted sensitivity of 17 mJy at 11.7 microns with a bandwidth of 2.4 microns. This translates into $10.5 < \lambda < 12.9$ microns and a sensitivity of about 5.3×10^4 photons m^{-2} sec^{-1}. The field of view of this instrument is about 20 arcmin, which translates into about 2.7×10^{-5} sr. In our case, it translates into an energy range of $0.096\ \mathrm{eV} < E_\gamma < 0.118\ \mathrm{eV}$ and into a photon flux of 3.7×10^{-5} photons m^{-2} sec^{-1} with a field of view of 1.48 sr.

The ALMA instrument [73] is sensitive in the mm spectrum; we will use a wavelength of 3 mm as representative.

Using Eq. (9.8) from the user's manual to get the sensitivity of the detector and Figs. 4–7 to get the temperature (70 K) and assuming an integration time of 1 hour, we calculate a sensitivity of about 8 photons $m^{-2}\,sec^{-1}$ for a frequency band from 84 to 105 GHz: 2.9 mm $< \lambda <$ 3.6 mm. This number is encouraging but one has to factor in the field of view of the instrument, which is about [Eqs. (3)–(4)] 53 arcseconds, which translates into 5.4×10^{-8} sr. Using scenario A in Table I, we would get about 100 photons $m^{-2}\,sec^{-1}$ within the same wavelength range, which translates into 0.00035 eV $< E_\gamma <$ 0.00043 eV with a field of view of $0.47\pi \sim 1.48$ sr.

If we consider instruments with wider fields of view, the Samuel Oschin Telescope [74] is high on the list with a very wide field of view at 4.6×3.6 degrees^2, which translates into about 4×10^{-3} sr. Its quoted sensitivity is $m = 20.4$, which translates into about 300 photons $m^{-2}\,sec^{-1}$ in the visible, assuming that about 10% of the Sun's energy is emitted in the visible where photons have an average energy of about 2 eV. Unfortunately our signal in the visible is at best 10^{-7} photons $m^{-2}\,sec^{-1}$ with a field of view of 1.48 sr.

Comparing the required flux from the instruments with the expected flux from the process, and taking the different opening angles or fields of view into consideration we see that we need a factor of about 2×10^{17} with New Horizon, 3.6×10^{15} for the VISIR instrument, 8×10^{13} for KEK, 2.2×10^6 for ALMA and 10^{12} for the Oschin instrument before our signal could be detected. The instruments that have a very wide field of view work in the visible and our signal is very poor in that frequency regime due to the very low energy of the collision between the solar wind and the DM particle. Things improve when we go to longer wavelengths: the field of view of the instruments is reduced, but our signal is greatly improved. The best opportunity seems to come from the ALMA instrument. With this instrument: we get 8 $m^{-2}\,sec^{-1}/5.4 \times 10^{-8}$ sr $= 1.5 \times 10^8$ $m^{-2}\,sec^{-1}\,sr^{-1}$ and our signal is about 65 $m - 2\,sec^{-1}\,sr^{-1}$ in the same bandwidth. We need to enhance our signal by a factor of about 2.2×10^6. We have three free parameters in our amplitude, namely $\lambda^2\Lambda^2/(m_{\text{exchange}}/0.1\text{ GeV})^4$ and the density of the dark matter particles in the vicinity of the Sun. We assume that all the mass of the dark matter density is carried by the heavy, colliding dark matter particles, at 2 GeV. The density of 0.3 GeV/cm^3 is rather well established, which also establishes our dark matter density. This leaves us with the $\lambda^2\Lambda^2/(m_{\text{exchange}}/0.1\text{ GeV})^4$ term. In order to get a factor of 2.5×10^6 with this expression, we could assume that the exchanged particle has a mass of only 2.5 MeV instead of 100 MeV. This would bring our signal to a detectable level at ALMA with couplings of order 1. We could say that the region of parameter space such that $\lambda^2\Lambda^2/(m_{\text{exchange}}/0.1\text{ GeV})^4 > 2.5 \times 10^6$ could be potentially excluded at ALMA if the signal is not observed. Again, it is a very difficult signal to observe as it would be a diffuse background, without a direct source.

There is another parameter that could enhance our signal. Up to this point, we have assumed that the dark matter particles are at rest in the Galaxy and their motion relative to the solar wind is due to the motion of the Sun through our Galaxy. This is a little limiting as there are scenarios where the DM particles have a speed of a few hundred km/ sec [46]. Clearly, such a velocity will have an effect on the production rate since this speed is comparable to the speed of the solar wind. We have verified that doubling the speed of the DM particles to 0.002 c, increases the cross section by a factor of about 2.2 when the collision is at an angle of less than 90° but the effect is smaller when the collision angle is larger: about 2 at 90° down to about 1.1 at 135°. Similar behavior is observed when the DM speed is increased to 0.003 c: the cross section is increased about fivefold when the collision angle is less than 90°, about 4.3 at 90° down to about 3 at 135°. When integrating over the cone, one could get an increase in the photon rates of about 2 if the speed of the DM particles is doubled and a factor of about 4 if it is tripled. This effect would not be sufficient to bring the photon flux to measurable levels in the visible range (New Horizon), nor in the micron range (VISIR), but it would have an impact in the mm (ALMA) and would increase the exclusion zone. One would then require $\lambda^2\Lambda^2/(m_{\text{exchange}}/0.1\text{ GeV})^4 > 10^6$ in order to reach measurable levels at ALMA and exclude a larger portion of parameter space.

Let us assume for simplicity that $\lambda = \Lambda$, then our constraint becomes $\lambda/(m_{\text{exchanged}}/0.1\text{ GeV}) < 0.032$ (or 0.04 if we assume 2.5×10^{-6} instead of 10^{-6}) In this case, if we push $m_{\text{exchanged}}$ down to 0.01 GeV, then $\lambda < 3.2 \times 10^{-3}$. Likewise, by pushing $m_{\text{exchanged}}$ down to 1 eV, then $\lambda < 3.2 \times 10^{-10}$ is reached and these limits are comparable to those obtained through a Yukawa model of interaction between the DM particle and a nucleon [75,76] or what is expected at the FCCee [77]. Similar bounds on couplings have also been calculated for axionlike particles at future colliders [78]. One can say that the process at hand is sensitive to light DM particles that can be exchanged between the solar wind particle and the heavier DM particles. In a model where several DM particles can coexist with very different masses, be stable and interact with each other and with the proton, the scenario that we consider here would be the dominant one. Indeed, a heavier exchange particle would reduce the t-channel amplitude and a lighter colliding particle would reduce the bremsstrahlung as a proton would interact very little with a very light DM particle and the energy emitted through bremsstrahlung would be negligible.

Reversing the situation, a scenario where the heavier DM particle couples to lighter dark particles would lead to their production through bremmstrahlung off the DM particle as it scatters off the solar wind, thereby increasing their

presence in our Solar System. This effect would be larger in close proximity of the Sun. Similarly, in a model similar to the one considered here, a proton could emit via bremsstrahlung a light dark matter particle [79].

There is also the interesting possibility that an electron could interact with the DM; such couplings have been considered before in the context of the 0.511 MeV emission from the center of the Galaxy [80,81] and the possibility of DM upscattering in the Sun [37]. This process should lead to results similar to what we have here and opens up the possibility of sensitivity to very small masses in the DM spectrum since the bremsstrahlung seems to be maximum when the colliding particles have about the same momentum and the electrons in the solar wind have a speed similar to that of the Sun in the Galaxy. A proposed future MeV gamma-ray telescope is expected to probe the MeV or sub-MeV DM mass range [82].

We have neglected cosmic magnetic fields, which would bend the solar wind and modify the colliding angles within the observation cone. Evaluating the effects of these fields on the spectrum would be interesting, but it is unlikely this could make the signal observable in the visible, for example. We have also neglected the effect of the Sun on the density of the DM. It is likely that the presence of the Sun would increase the density of the DM particles in its vicinity and as most of the spectrum is produced relatively close to the Sun, this would tend to increase the counting rate observed, but likely not enough to gain several orders of magnitude. When considering the spectrum at longer wavelengths however (in the mm or cm range) and assuming that the spectrum keeps a slope similar to what we have calculated here, then these effects could make a difference in the observable spectrum. We have assumed that the Sun moves towards the Earth (or the observation points) in its motion around the Galaxy. Taking the real motion of the Sun into account could have a small effect on our results and bring some periodicity to our signal. A more precise calculation (finer angular and energy bins and finer sampling mesh) is necessary in order to assess the importance of these effect at very low photon energy as well as a precise modeling of the cosmos in this regime [83].

X. CONCLUSIONS

We have considered the scattering of the solar wind off DM particles that might be populating our Solar System. We allowed the scattered proton to emit a photon through bremmstrahlung and calculated the spectrum that one would observe either at 1 or 50 au from the Sun. We have assumed a uniform DM density in our region of the Galaxy and neglected the effects of cosmic magnetic fields on the solar wind. We have found that the rates are very small in general and could not explain the excess luminosity observed recently by the New Horizon probe. Extrapolating our results down to 0.01 eV is reasonable and indicates that the rates are still very small with the parameters we used. Extrapolating further to mm wavelengths, we find that a telescope like ALMA could set interesting limits in our parameter space if we push the mass of the exchanged particle down to eV level as this forces the couplings to the 10^{-10} range. A more precise numerical calculation would be required to confirm this behavior of the photon flux down to very low photon energies.

The scenario that we have considered and appears to be the most promising is that of a DM particle whose mass is about $2\,m_{\text{proton}}$ interacting with a proton via the exchange of a much lighter DM. This opens up the possibility of bremsstrahlung of the lighter DM particle off the heavier DM particle as the latter scatters off a proton, thereby increasing the abundance of the lighter DM particle.

Considering bremsstrahlung emission from the scattering of electrons off DM particles also opens up the possibility of exploring small mass regime in the DM sector since the bremsstrahlung seems to be maximum when the momentum of the colliding particles are about the same and the solar wind has a speed similar to that of the Sun in the Galaxy. In this particular scenario, one could have only one very light DM particle that interacts and is exchanged with the electron.

ACKNOWLEDGMENTS

I want to thank my colleagues Chérif Hamzaoui and Manuel Toharia for stimulating discussions and my colleagues from the Atlas Collaboration at the Physics Department at Université de Montréal for the use of their computers. I also want to thank T. Lauer (New-Horizon), M.v-d-Ancker (Visir), and A. Hales (Alma) for discussions about the sensitivity of their instruments and any potential misunderstanding of their explanations is entirely mine.

[1] E. Aprile *et al.*, Phys. Rev. D **102**, 072004 (2020).
[2] H. An, M. Pospelov, J. Pradler, and A. Ritz, Phys. Rev. D **102**, 115022 (2020).
[3] S. Vagnozzi, L. Visinelli, P. Brax, A.-C. Davis, and J. Sakstein, arXiv:2103.15834.
[4] M. Dutta, S. Mahapatra, D. Borah, and N. Sahu, arXiv:2101.06472.

[5] J. Billard, M. Boulay, S. Cebrian, and L. Covi, arXiv:2104.07634.
[6] M. Szydagis, C. Levy, G. M. Blockinger, A. Kamaha, N. Parveen, and G. R. C. Rischbieter, Phys. Rev. D **103**, 012002 (2021).
[7] A. E. Robinson, arXiv:2006.13278.
[8] E. Aprile *et al.* (XENON Collaboration), J. Cosmol. Astropart. Phys. 11 (2020) 031.
[9] D. S. Akerib *et al.* (LUX Collaboration), Phys. Rev. D **101**, 052002 (2020).
[10] A. H. Abdelhameed *et al.* (CRESST Collaboration), Phys. Rev. D **100**, 102002 (2019).
[11] H. Kluck (CRESST Collaboration), J. Phys. Conf. Ser. **1468**, 012038 (2020).
[12] X. Ren *et al.* (PANDA Collaboration), Phys. Rev. Lett. **121**, 021304 (2018).
[13] J. Yang *et al.* (PANDA Collaboration), arXiv:2104.14724.
[14] H. An, M. Pospelov, J. Pradler, and A. Ritz, Phys. Lett. B **747**, 331 (2015).
[15] G. Prézeau, A. Kurylov, M. Kamionsky, and P. Vogel, Phys. Rev. Lett. **91**, 231301 (2003).
[16] D. Hooper and S. M. McDermott, Phys. Rev. D **97**, 115006 (2018).
[17] E. Behnke *et al.* (PICASSO Collaboration), Astropart. Phys. **90**, 85 (2017).
[18] M. Lafrenière, Thèse de Doctorat, Département de physique, Université de Montréal, 2016.
[19] C. Amole *et al.* (PICO Collaboration), Phys. Rev. D **100**, 022001 (2019).
[20] C. B. Krauss (PICO Collaboration), J. Phys. Conf. Ser. **1468**, 012043 (2020).
[21] R. Bernabei *et al.*, Int. J. Mod. Phys. A **22**, 3155 (2007).
[22] M. Ibe, W. Nakano, Y. Shoji, and K. Suzuki, J. High Energy Phys. 03 (2018) 194.
[23] N. F. Bell, J. B. Dent, J. L. Newstead, S. Sabharwal, and T. J. Weiler, Phys. Rev. D **101**, 015012 (2020).
[24] V. S. Flambaum, L. Su, L. Wu, and B. Zhu, arXiv:2012.09751.
[25] J. A. Dror, G. Elor, R. McGehee, and T.-T.Yu, Phys. Rev. D **103**, 035001 (2021).
[26] C. Kouvaris and J. Pradler, Phys. Rev. Lett. **118**, 031803 (2017).
[27] M. J. Dolan, F. Kahlhoefer, and C. McCabe, Phys. Rev. Lett. **121**, 101801 (2018).
[28] R. Essig, J. Mardon, and T. Volansky, J. High Energy Phys. 05 (2016) 046.
[29] B. V. Lehmann and S. Profumo, Phys. Rev. D **102**, 023038 (2020).
[30] G. D. Starkman and D. N. Spergel, Phys. Rev. Lett. **74**, 2623 (1995).
[31] G. Grilli di Cortona, A. Messina, and S. Piacentini, J. High Energy Phys. 11 (2020) 034.
[32] W. Yin, Eur. Phys. J. Web Conf. **208**, 04003 (2019).
[33] T. Bringmann and M. Pospelov, Phys. Rev. Lett. **122**, 171801 (2019).
[34] J. Alvey, M. Campos, M. Fairbairn, and T. You, Phys. Rev. Lett. **123**, 261802 (2019).
[35] M. Klasen, M. Pohl, and G. Sigi, Prog. Part. Nucl. Phys. **85**, 1 (2015).
[36] N. Vinyoles, A. Serenelli, F. L. Villante, S. Basu, J. Redondo, and J. Isern, J. Cosmol. Astropart. Phys. 10 (2015) 015.
[37] H. An, M. Pospelov, J. Pradler, and A. Ritz, Phys. Rev. Lett. **120**, 141801 (2018).
[38] R. K. Leane and J. Smirnov, Phys. Rev. Lett. **126**, 161101 (2021).
[39] V. Gluscevic and K. K. Boddy, Phys. Rev. Lett. **121**, 081301 (2018).
[40] Y. Ali-Haïmoud, J. Chuba, and M. Kamionskowski, Phys. Rev. Lett. **115**, 071304 (2015).
[41] K. Maamari, V. Gluscevic, K. K. Boddy, E. O. Nadler, and R. H. Wechsler, Astrophys. J. Lett. **907**, L46 (2021).
[42] S. Afach *et al.*, arXiv:2102.13379.
[43] A. Derevianko and M. Pospelov, Nat. Phys. **10**, 933 (2014).
[44] M. Bauer, M. Heiles, M. Neubert, and A. Thamm, Eur. Phys. J. C **79**, 74 (2019).
[45] H. Mies, C. Schreb, and P. Schwaller, J. High Energy Phys. 04 (2021) 049.
[46] J. I. Read, J. Phys. G **41**, 063101 (2014).
[47] C. J. Copi and L. M. Krauss, Phys. Rev. D **63**, 043507 (2001).
[48] P. Salucci, F. Nesti, G. Gentile, and C. F. Martins, Astron. Astrophys. **523**, A83 (2010).
[49] H. Bethe and W. Heitler, Proc. R. Soc. A **146**, 83 (1934).
[50] J. D. Jackson, *Classical Electrodynamics* 2nd ed. (Wiley, New York, 1975).
[51] P. Talukdar, F. Myhrer, and U. Raha, Eur. Phys. J. A **54**, 195 (2018).
[52] U. Eichmann and W. Greiner, J. Phys. G **23**, L65 (1997).
[53] T. S. Biro, K. Nita, A. L. DePaoli, W. Bauer, W. Cassing, and U. Mosel, Nucl. Phys. **A475**, 579 (1987).
[54] G. Baur and A. Leuschner, Eur. Phys. J. C **8**, 631 (1999).
[55] W. Zhu, Nucl. Phys. **B953**, 114958 (2020).
[56] M. Cirelli, P. D. Serpico, and G. Zaharijas, J. Cosmol. Astropart. Phys. 11 (2013) 035.
[57] J. B. Dent, B. Dutta, J. L. Newstead, A. Rodriguez, I. M. Shoemaker, and Z. Tabrizi, arXiv:2012.07930.
[58] L. Su, L. Wu, and B. Zhu, arXiv:2105.06326.
[59] J. D. Bjorken and S. D. Drell, *Relativistic Quantum Mechanics* (McGraw-Hill, New York, 1964), Vol. 1.
[60] M. E. Peskin and D. V. Schroeder, *An Introduction to Quantum Field Theory* (Addison Wesley, New York, 1995).
[61] F. Gross, *Relativistic Quantum Mechanics and Field Theory* (Wiley Interscience, New York, 1993).
[62] R. Hagedorn, *Relativistic Kinematics* (Benjamin/Cummings, London, 1963).
[63] V. D. Barger and R. J. N. Phillips, *Collider Physics* (Addison Wesley, New York, 1987).
[64] A. Savitzky and M. J. E. Golay, Anal. Chem. **36**, 1627 (1964).
[65] W. Herr and B. Muratori, Concept of luminosity, *CERN Accelerator School and DESY Zeuthen: Accelerator Physics* (2003), pp. 361–377.
[66] H. Burkhardt and P. Grafstrom, Absolute luminosity from machine parameters, CERN Report No. CERN-LHC-PROJECT-REPORT-1019, 2007.
[67] M. Pospelov, A. Ritz, and M. Voloshin, Phys. Lett. B **662**, 53 (2008).

[68] K. Schutz and T. R. Statyer, J. Cosmol. Astropart. Phys. 01 (2015) 21.
[69] A. Dedes, I. Giomataris, K. Suxho, and J. D. Vergados, Nucl. Phys. **B826**, 148 (2010).
[70] T. R. Lauer *et al.*, Astrophys. J. **906**, 77 (2021).
[71] VISIR manual: https://www.eso.org/sci/facilities/paranal/instruments/visir/doc/VLT-MAN-ESO-14300-3514_2020-03-03.pdf.
[72] KEK manual: https://www2.keck.hawaii.edu/observing/kecktelgde/ktelinstupdate.pdf (page 18).
[73] ALMA manual: https://almascience.nrao.edu/documents-and-tools/cycle8/alma-technical-handbook.
[74] C. Baltay *et al.*, Publ. Astron. Soc. Pac. **119**, 1278 (2007).
[75] M. C. Digman, C. V. Cappiello, J. F. Beacom, C. M. Hirata, and A. H. G. Peter, Phys. Rev. D **100**, 063013 (2019).
[76] S. Knapen, T. Lin, and K. M. Zurek, Phys. Rev. D **96**, 115021 (2017).
[77] S. Knapen and A. Thamm, Eur. Phys. J. Plus **136**, 936 (2021).
[78] M. Bauer, M. Heiles, M. Neubert, and A. Thamm, Eur. Phys. J. C **79**, 74 (2019).
[79] N. F. Bell, Y. Cai, J. H. Dent, R. K. Leane, and T. Weiler, Phys. Rev. D **96**, 023011 (2017).
[80] R. Bernabei *et al.*, Phys. Rev. D **77**, 023506 (2008).
[81] J. F. Beacom, N. F. Bell, and G. Bertone, Phys. Rev. Lett. **94**, 171301 (2005).
[82] A. Coogan, A. Moiseev, L. Morrison, and S. Profumo, arXiv:2101.10370.
[83] D. Gaggero and M. Valli, Adv. High Energy Phys. **2018**, 3010514 (2018).